Carbohydrate Polymers 177 (2017) 178–186

Contents lists available at ScienceDirect

Carbohydrate Polymers

journal homepage: www.elsevier.com/locate/carbpol

Self-aggregates of 3,6-*O*,*O*'-dimyristoylchitosan derivative are effective in enhancing the solubility and intestinal permeability of camptothecin

Daniella S. Silva[a], Andreia Almeida[b], Fabíola G. Prezotti[c], William M. Facchinatto[a], Luiz A. Colnago[d], Sérgio P. Campana-Filho[a], Bruno Sarmento[b,e,*]

[a] São Carlos, Institute of Chemistry, University of Sao Paulo, Avenida Trabalhador São-Carlense, 400-13560-970, São Carlos, SP, Brazil
[b] Institute for Research and Innovation in Health (i3S) and Institute of Biomedical Engineering (INEB), University of Porto, Rua Alfredo Allen, 208, 4200-393 Porto, Portugal
[c] Graduate Program in Pharmaceutical Sciences, Department of Drugs and Pharmaceuticals, School of Pharmaceutical Sciences, São Paulo State University—UNESP, Rodovia Araraquara–Jaú, Km 1, 14801-902, Araraquara, SP, Brazil
[d] Embrapa Instrumentação, Rua XV de Novembro 1452, 13560-970, São Carlos, Brazil
[e] IIFACTS—Institute for Research and Advanced Training in Health Sciences and Technologies, Rua Central de Gandra 1317, 4585-116 Gandra, Portugal

ARTICLE INFO

Keywords:
Chitosan
Amphiphilic chitosan derivative
Polymeric micelles
Camptothecin
Oral drug delivery

ABSTRACT

The aim of this work was to investigate the potential of a new 3,6-*O*,*O*'-dimyristoyl derivative amphiphilic chitosan (DMCh), in improving the solubility of camptothecin (CPT), a hydrophobic anticancer drug, and its potential oral delivery. FTIR, ^{1}H NMR and solid-state ^{13}C NMR spectroscopy were used to characterize DMCh and to determine its average degree of substitution ($\overline{DS}$ = 6.8%). DMCh/CPT micelles size ranged from (281–357 nm), zeta potential (+32–50 mV) of encapsulation efficiency of 42–100%. The *in vitro* cell viability showed that DMCh/CPT micelles were able to reduce the toxicity of CPT. The *in vitro* permeability of CPT through Caco-2 and Caco-2/HT29-MTX intestinal models was increased up to ten fold when formulated into DMCh micelles, underlining the mucoadhesive properties of the nanocarrier. DMCh/CPT micelles are able to enhance CPT solubility and bioavailability while reduce its cytotoxicity, showing the great potential for intestinal delivery of hydrophobic drugs.

1. Introduction

Camptothecin (CPT), an anticancer agent extracted from *Camptotheca acuminate*, exhibits a strong antitumor activity against a large spectrum of tumors. Its action is attributed to the inhibition of the nuclear enzyme topoisomerase I and depends on the α-hydroxycarbonyl group present at the lactone ring (Gonzalez-alvarez, Rodríguez-berna, Mangas-sanju, & García-gim, 2014; Huarte et al., 2016; Pagano et al., 2015). Nevertheless, the therapeutic application of CPT is severely limited by its low solubility in aqueous media and high toxicity, and because of the inactivation of the lactone ring inactivation due to the high reactivity of the α-hydroxycarbonyl group. Indeed, when exposed to physiological pH conditions, the lactone ring of CPT can undergo hydrolysis, and an equilibrium between the closed-ring lactone moiety and the open-ring carboxylic acid form can exist (Concheiro, 2010; Gao et al., 2008; Kolhatkar, Swaan, & Ghandehari, 2008; Laskar, Samanta, Kumar, & Dey, 2014). The carboxylic acid form of CPT is pharmacologically ineffective and it is responsible for the occurrence of highly toxic effects, such as myelosuppression, hemorrhagic cystitis and diarrhea, excluding its clinical use. In addition, some studies reported that the carboxylate form of CPT has high affinity for human serum albumin, which provokes the shift of the equilibrium between the lactone and the carboxylic form of CPT toward the latter one (Mi & Burke, 1994; Opanasopit et al., 2005).

The advance of new proposals focused on solving problems related to limitations in the use of CPT has led to the development of new formulations, among which the systems based on liposomes, dendrimers, polymer conjugates and polymer-based micelles capable to improve the efficacy of CPT toward malignant cells while reducing its toxicity, enhancing permeability and retention effect (Kawano, Watanabe, Yamamoto, & Yokoyama, 2006; Maeda, 2001). In particular, polymer-based micelles have been considered as promising systems because of their characteristics in drug loading, release, delivery, and stability (Zhang, Ding, Lucy, & Ping, 2007a, Zhang, Ding, Yu (Lucy), & Ping, 2007b). Additionally, polymeric micelles composed by amphiphilic polymers assume a core-shell architecture in aqueous

* Corresponding author at: Institute for Research and Innovation in Health (i3S) and Institute of Biomedical Engineering (INEB), University of Porto, Rua Alfredo Allen, 208, 4200-393 Porto, Portugal.
E-mail addresses: bruno.sarmento@ineb.up.pt, brunocsarmento@hotmail.com (B. Sarmento).

http://dx.doi.org/10.1016/j.carbpol.2017.08.114
Received 13 April 2017; Received in revised form 7 August 2017; Accepted 27 August 2017
Available online 31 August 2017
0144-8617/

media, the water-insoluble drug being encapsulated into the hydrophobic core of the polymeric micelles by covalent coupling or physical interactions, which promotes the solubilization of the drug and prevents its degradation (Duan et al., 2010). Furthermore, the hydrophilic shell prevents the recognition of such polymeric micelles by the immune system, prolonging the drug circulation and improving the drug stability in aqueous medium (Hyun et al., 2008). In the last decades, micelles based in amphiphilic block-like copolymers have been exploited for encapsulation/release of drugs, especially in the case of water insoluble drugs. However, the industrial development of these systems is still very limited due to the difficulties of preparation and to high costs (Ebrahim Attia et al., 2011).

In order to avoid the difficulties related to the preparation of copolymers, chitosan has been considered as a promising agent with potential applications in the biomedical and pharmaceutical area. This cationic biopolymer exhibits interesting biological activities, such as biocompatibility, biodegradability, mucoadhesiveness, antimicrobial activity and antioxidant properties, and it is can be chemically modified by derivatization of its numerous hydroxyl and amino groups (Delmar & Bianco-Peled, 2016; Shrestha et al., 2014; Unsoy, Khodadust, Yalcin, Mutlu, & Gunduz, 2014; Xu, Strandman, Zhu, Barralet, & Cerruti, 2015).

Thus, different amphiphilic chitosan derivatives have been proposed as carriers of hydrophobic drugs, such as *N*-(2,3-dihydroxypropyl)–chitosan–cholic acid (Pan et al., 2013), chitosan-grafted-polylactide (Di Martino & Sedlarik, 2014), *N*-octyl-*N*-trimethyl chitosan (Zhang et al., 2007a,b), *N*-propyl-*N*-methylene phosphonic chitosan (Zuñiga, Debbaudt, Albertengo, & Rodríguez, 2010), stearic acid-grafted chitosan oligosaccharide (Ye et al., 2008), *N*-naphthyl-*N,O*-succinyl chitosan, *N*-octyl-*N,O*-succinyl chitosan and *N*-benzyl-*N,O*-succinyl chitosan (Woraphatphadung et al., 2016).

Although different types of carriers for anticancer drugs have been studied, modest progress has been achieved in the treatment of cancer due to lack of selectivity against cancer cells (Ge, Ma, & Li, 2016; Wang et al., 2011). Additionally, the therapeutic action of a single drug has been limited. However, the combination of drugs has attracted the attention of researchers, with two or more anticancer agents being combined through co-administration. This type of therapy focuses on different signaling pathways in tumor cells, surpassing the resistance mechanisms of malignant cells (Feng et al., 2014; Greco & Vicent, 2009; Parhi, Mohanty, & Sahoo, 2012; Wu, Wang, Zhuo, & Cheng, 2014; Zhao et al., 2015). Therefore, knowing how a drug carrier behaves for different types of chemotherapeutic agents, with different mechanisms of action and physicochemical properties, is an encouraging approach. The 3,6-*O,O*'-dimyristoyl chitosan derivative (DMCh) has been studied in our previous work for the encapsulation of paclitaxel (Silva et al., 2017). The promising results previously obtained motivated our research group to evaluate the ability of this new polymer to act as a drug delivery system for CPT. The properties of the DMCh derivative and the characteristics of the CPT-loaded drug-loaded micelles (DMCh/CPT), such as mean particle size, zeta potential, surface morphology, encapsulation efficiency and drug release behaviors were investigated. The *in vitro* toxicity of DMCh/CPT2 micelles was evaluated using Caco-2 (clone C2BBe1) and HT29-MTX cell lines, the same cell lines being used in the study of intestinal permeability. Therefore, the potential of the DMCh micelles as a CPT carrier was studied by investigating the application this system to the oral absorption of the drug.

2. Experimental

2.1. Materials

Commercial chitosan, extracted from fly larvae (Cheng Yue Planting Co. Ltd.; Chang/China) was characterized with respect to viscosity-average molecular weight ($\overline{Mv}$ = 87,000 g/mol) and average degree of acetylation ($\overline{DA}$ = 5%) by carrying out viscosity measurements and ^{1}H NMR spectroscopy as reported elsewhere (Fiamingo, Delezuk, Trombotto, David, & Campana-Filho, 2016). All other reagents and solvents were used as acquired, i. e. without any purification.

Cell culturing reagents: Caco-2 cells (clone C2BBe1) were obtained from American Type Culture Collection (ATCC, USA), and HT29-MTX cell line was kindly provided by Dr. T. Lesuffleur (INSERMU178, Villejuif, France). Dulbecco's Modified Eagle Medium (DMEM, Lonza), supplemented with 10% (v/v) fetal bovine serum (FBS) (Merck Millipore), 1% (v/v) penicillin (100 UI/mL, Merck Millipore) and streptomycin (100 µg/mL, Merck Millipore) and 1% (v/v) nonessential amino acids (NEAA, Merck Millipore). 3-(4,5-dimethylthiazol-2-yl)-2,5-diphenyltetrazolium bromide (MTT) and dimethyl sulfoxide (DMSO) from Sigma Aldrich, Triton X-100 1% (Spi-Chem) (Sgorla et al., 2016).

2.2. Characterization of 3,6-O,O'-dimyristoyl chitosan

The preparation of 3,6-*O,O*'-dimyristoyl chitosan (DMCh) was carried out by reacting chitosan with myristoyl chloride in the presence of MeSO3H as reported earlier (Silva et al., 2017). Infrared spectra were registered from 32 scans with resolution of 4 cm-1 by using IRAffinity-1 Shimadzu spectrometer. 1H NMR spectroscopy was conducted to confirm the chemical structure of DMCh and to determine its average degree of substitution (Silva et al., 2017). Solid-state ^{13}C NMR analysis was carried out by using a Bruker Avance 400 spectrometer, with a Bruker 4-mm magical angle spinning (MAS) double-resonance probe head at 100.5 MHz (^{13}C) and 400.0 MHz (^{1}H). It was used a pneumatic system to control the spinning frequency at 12 kHz (± 1 Hz). Field strengths corresponding to π/2 pulses lengths of 4 µs (^{13}C) and 3.5 µs (^{1}H) were used for the spin-lock cross-polarization transfer, and 70 kHz for proton decoupling. The ^{13}C quantitative spectra of the chitosan and DMCh were obtained through the recently proposed MultiCP (multiple cross-polarization) excitation method (Johnson & Schmidt-Rohr, 2014).

The average degree of acetylation ($\overline{DA}$) of chitosan was obtained from the relative signal intensity of methyl carbon (ICH3) and glucopyranose ring carbons (IC1, IC2, IC3, IC4, IC5, IC6), according to the literature (Heux, Brugnerotto, Desbrières, Versali, & Rinaudo, 2000; Ottøy, Vårum, & Smidsrød, 1996). The average degree of substitution ($\overline{DS}$) of DMCh was obtained from the relative intensities of DMCh C═O carbons (161 − 169 ppm), and C1 carbon of glucopyranose ring (100–116 ppm). Both parameters, i.e. $\overline{DA}$ of chitosan and $\overline{DS}$ of DMCh, were calculated by fitting Gaussian functions to reduce the error arising from signal-to-noise ratio (Heux et al., 2000).

The CAC was determined by using the conductivity method. Thus, the conductivity of DMCh solutions as a function of polymer concentration (1×10^{-6} mg/mL ≤ Cp ≤ 1 mg/mL) at 25 °C under continuous stirring was measured by using a Consort C863 conductivity meter.

2.3. Preparation of CPT-loaded DMCh micelles

Briefly, DMCh was dissolved in 0.1 M acetic acid at Cp = 1 mg/mL while CPT was dissolved in dimethyl sulfoxide (DMSO) and its solution (Cp = 1 mg/mL) was added to the DMCh solution to result in polymer:CPT mass ratio in the range 1.0% − 3.0% (50 µg/ mL to 150 µg/ mL of CPT). The solution containing DMCH and CPT was kept under magnetic stirring at 300 rpm, for 2 h at 25 °C, freezed at −80 °C and lyophilized to remove the solvent The dried product was resuspended in 5 mL of 0.1 M acetic acid and the solution was sonicated for 5 min using a probe-type sonicator (Vibra-cell, Sonics Material INC. Danbury, USA) in iced water. Finally, the solution was centrifuged (Thermo Scientific Heraeus Megafuge 1.0R) at 5000 rpm for 10 min to remove the non-encapsulated CPT.

2.4. Micelles size and morphology

The mean particle size and dispersity index of DMC micelles were

determined from the dynamic light scattering (DLS) measurements and zeta potential by electrophoretic light scattering (ELS), using a ZetaSizer Nano ZS equipment (Malvern, UK). Three replicates of each formulation were produced and analysed. Transmission electron microscopy (TEM) measurements were performed using a JEOL JEM 1400 TEM microscope (Tokyo, Japan) and the images were digitally recorded using a Gatan SC 1100 ORIUS CCD camera (Warrendale, PA, USA).

2.5. Drug encapsulation efficiency (EE%)

The drug encapsulation efficiency (EE%) was determined by indirect method. The non-encapsulated CPT was separated from the micelles by centrifugation at 5000 rpm for 10 min, the free CPT was dissolved in DMSO/H_2O (9:1) and quantified by measuring the absorbance of the CPT solution at 370 nm by using a UV–vis spectrophotometer (Duan et al., 2010; Hyun et al., 2008; Opanasopit, Ngawhirunpat, & Chaidedgumjorn, 2006; Opanasopit, Ngawhirunpat, Rojanarata, Choochottiros, & Chirachanchai, 2007). The amount of CPT loaded into the DMCh micelles was determined by the difference between the amount of drug added in the preparation of CPT loaded micelles and the content of free drug. The EE% was calculated from the ratio between the amount of loaded drug and the total amount of drug used in the experiment, according to Eq. (1):

$$EE\% = \frac{(CPT_{total} - CPT_{free})}{CPT_{total}} \times 100 \quad (1)$$

where CPT_{total} is the total amount of drug used in the preparation of DMCh/CPT micelles, and CPT_{free} is the amount of free drug. Tests were performed in triplicate.

2.6. In vitro drug release study

In order to study the *in vitro* release profile of CPT from DCMh/CPT2 micelles, two different conditions were tested, simulating the different pH values found along the gastrointestinal tract after oral administration. The test was carried out using simulated gastric fluid (SGF; 0.1N HCl; pH 1.2) for the first 2 h and simulated intestinal fluid (SIF; PBS; pH 6.8) for the rest of the experiment. Tween 80® (1% v/v) was added to both simulated fluids to ensure sink conditions. An aliquot (5 mL) of the suspension of DMCh/CPT micelles containing 70 μg of CPT was introduced into dialyses bags (10 KDa cut-off, Thermo Scientific), dialyzed against 40 mL of the release medium (SGF or SIF) and at predetermined time (0.25, 0.5, 1, 2, 4, 8, 12, 24 and 48 h), 1 mL of release medium was removed and the same volume of fresh simulated fluid was added. Also, for comparison purposes, the same amount of free CPT (70 μg) was tested. All samples were placed in an orbital shaker at 37 °C and 100 rpm and the drug released was determined by HPLC analysis. Each experiment was carried out in triplicate and the result is present as mean and corresponding standard deviations (mean ± SD).

2.7. In vitro studies

2.7.1. Cytotoxicity assay

The toxicity of CPT-loaded DMCh micelles and free CPT was assessed in Caco-2 and HT29-MTX cell lines, using the MTT reagent. Cells were seeded (200 μL) into wells of 96-well plates at a density of 1×10^4 cells/well for HT29-MTX cell line and 2×10^4 cells/well for Caco-2 and then they were incubated overnight at standard condition to reach exponential growth prior to the assay test. At the following day, the medium was removed and the cells were washed twice with 200 μL of phosphate buffered saline (PBS). After, the cells were treated with free CPT and CPT-loaded micelles in the concentration range of 0.001–1000 μg/mL. The positive control was DMEM and negative control was 1% (w/v) Triton X-100. The cultured cells were incubated for 24 h in the presence of different concentrations of samples. Then, samples were removed and 200 μL of the MTT reagent (0.5 mg/mL) were added followed by an incubation period of 4 h. After, the MTT was removed and 200 μL of DMSO were added to each well to dissolve the formazan crystals. The plates were vigorously shaken for 10 min inside the microplate reader before the relative color intensity was measured at 570 nm and taking the absorbance at 630 nm as a reference, by using a microplate reader (Synergy 2, Biotek Instruments Ltda, USA).

2.7.2. Permeability studies

Monoculture model of Caco-2 cells and co-culture model of Caco-2:HT29-MTX at the proportion 90:10 were seeded on 6-well Transwell™ cell culture inserts (transparent PET, 3 μm pore size, 4.67 cm^2, Corning Life Sciences), as previously established by us (Antunes, Andrade, Araújo, Ferreira, & Sarmento, 2013; Araújo & Sarmento, 2013). The cell lines with passage 58–60 to Caco-2 and 35–37 to HT29-MTX were seeded on the apical compartment at a density of 4.5×10^5 cells/cm^2 per insert. Cells were grown for 21 days until reaching confluency and the medium was changed every 2 days.

Before permeability experiments, cells were washed twice with pre-warmed Hank's buffered salt solution (HBSS) and then replaced with new HBSS and allowed to equilibrate for 30 min at 37 °C at 100 rpm. In the basolateral side, it was added HBSS with Tween 80® (1% v/v) in order to maintain the sink conditions. Permeability studies of CPT-loaded micelles and free CPT (75 μg/mL) were run at the same conditions during 3 h and samples were collected at different time (15, 30, 45, 60, 90, 120 and 180 min). Each sample was taken from the basolateral side of the Transwell™ cell culture insert and the same volume of pre-warmed HBSS was added to replace the withdrawn volume. The cell monolayers integrity was measured at the beginning, during and after the experiment, using an epithelial voltohmmeter EVOM2® with chopstick electrodes (World Precision Instruments, Sarasota, FL, USA). The permeability results were expressed as percentage of permeability and apparent permeability (P_{app}). P_{app} was calculated using the following Eq. (2):

$$P_{app} = \frac{\Delta Q}{A \times C_0 \times \Delta t} \quad (2)$$

where C_0 is the initial concentration in the apical side of the Transwell™ (μg/mL), A is the surface area of the insert (cm^2), Δt is the time during which experiment occurred (seconds) and ΔQ is the amount of compound detected in the basolateral side (μg). The TEER values, expressed in percentage, were normalized by subtracting the resistance value of the blank insert. All experiments were performed in triplicate and the CPT was quantified by HPLC as described before (Martins et al., 2012).

2.8. Statistical analysis

The experiments were performed in triplicate and are represented as mean ± standard deviation (SD). A two-way ANOVA with Bonferroni multiple/post hoc group comparisons was used to analyze the cytotoxicity and apparent permeability data. GraphPadPrism software Inc., USA, was used, and the level of significance was set at probabilities of $^*p < 0.05$, $^{**}p < 0.01$, and $^{***}p < 0.001$.

3. Results and discussions

3.1. Characterization of 3,6-O,O'-dimyristoyl chitosan

The successful synthesis of DMCh was confirmed by the presence of an intense band at 1740 cm^{-1} in its FTIR spectrum, which is attributed to axial deformation of carbonyl ester, resulting from the *O*-acylation of chitosan (Pavinatto, Souza, Pavinatto, Campana-Filho, & Oliveira, 2014; Tong, Wang, Xu, Chua, & He, 2005). The other characteristic bands in the spectrum of DMCh are assigned as follows: 3500 cm^{-1}–3300 cm^{-1} (OH stretching overlapped with NH stretching), 3000–2780 cm^{-1} (CH axial stretching); 1670–1650 cm^{-1} (amide I band, CO axial stretching of acetyl groups); 1600–1500 cm^{-1}

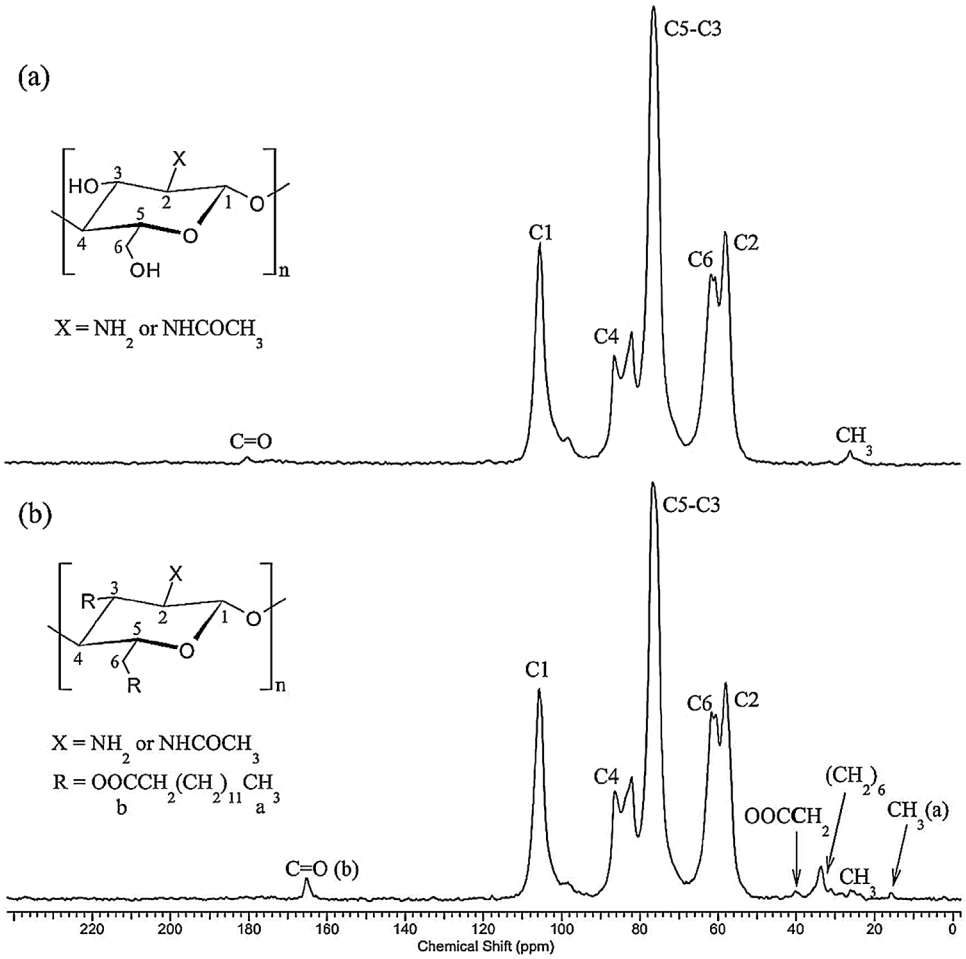

Fig. 1. Solid-state ^{13}C NMR spectra of chitosan (a) and DMCh (b) samples.

(amide II band, angular deformation of N—H) 1380 and 1370 cm^{-1} (asymmetric C—H bending in CH_3 groups); 1320–1300 cm^{-1} (C—N axial stretching, amide III) and 1070–1060 cm^{-1}, due to the axial deformation of C—O—C (Choi, Kim, Pak, Yoo, & Chung, 2007; Jiang, Quan, Liao, & Wang, 2006; Pavinatto et al., 2014).

In the ^1H NMR spectrum of DMCh the characteristic peaks of acyl group are observed at 0.9, 1.3, 1.7, 2.3 and 3.2 ppm and attributed to the hydrogen atoms of CH_3, CH_2, CH_2 (β) and CH_2 (α) moieties. The peaks at 3.0–4.5 ppm refer to the hydrogens of carbons 2–6 of the glucopyranose ring of chitosan (Badawy et al., 2005; Badawy et al., 2004; Choi et al., 2007; Hirano, Yamaguchi, & Kamiya, 2002; Hu et al., 2007). The ^1H NMR spectroscopy was used to determine the average degree of substitution of DMCh as $\overline{DS}$ = 6.8% while the measurements of conductivity allowed the determination of the critical aggregation concentration as CAC = 8.9×10^{-3} mg/mL as reported in our previous study (Silva et al., 2017).

The solid-state ^{13}C NMR spectra of chitosan and DMC are shown in Fig. 1. Despite de Gaussian function fitting, the weak and broad C=O peak at 180.6 ppm due to acetamide group leads to an unreliable quantitative analysis of $\overline{DA}$. However, the Gaussian fitting of the CH_3 signal, observed at 26 ppm, strongly reduces the low signal-to-noise systematic error. Thus, the average degree of acetylation of chitosan was determined as $\overline{DA} \approx 6.5\%$, in close agreement with the previous work (Silva et al., 2017). The chemical shifts of the signals due to the carbons of glucopyranose ring of chitosan (Fig. 1a) are in agreement with the literature, including the characteristic doublet of C4, observed at ≈ 82–88 ppm (Heux et al., 2000). The main signals due to chitosan carbon atoms are also observed at approximately the same chemical shift in the ^{13}C NMR spectrum of DMCh while the signals of C=O, CH_2 and CH_3 pertaining to myristoyl moieties are observed at 165 ppm, 20–35 ppm and at 15 ppm, respectively. Thus, owing to the presence of numerous $-CH_2-$ groups in the myristoyl moieties of DMCh, an intense and sharp signal is observed at approximately 30 ppm. Due to the overlapping of signals in the region 15 − 45 ppm, the intensity of the signals of the CH_3 and the $-CH_2-$ groups cannot be used for the determination of $\overline{DS}$. Therefore, it has been determined from the intensity of the signal due to the carbonyl group of DMCh (≈ 165 ppm) taking the signal due to C1 (≈105.7 ppm) as the reference, resulting in $\overline{DS} \approx 6.0\%$, in close agreement with our previous work (Silva et al., 2017).

3.2. Average size and morphology of DMCh micelles

The experimental data concerning the average size, dispersity (PDI) and zeta potential of empty and CPT-loaded DMCh micelles (Table 1) reveal that the encapsulation of CPT did not affect the mean particle size of the micelles ($p < 0.05$), which ranged in the interval 281 nm–357 nm. Additionally, regardless of the presence and concentration of CPT, the histograms of DMCh micelles (Fig. 2), representative of the other samples. The measurements of zeta potential allowed the evaluation of the contribution of repulsive electrostatic forces to stabilize the DMCh/CPT micelles. Accordingly, such measurements showed largely positive values of zeta potential (32 mV–50 mV), which are attributed to the presence of ammonium groups in the hydrophilic shell of DMCh micelles resulting from the protonation of amino groups pertaining to 2-amino-2-deoxy-D-glucopyranose units present in the polymer chains. Indeed, as the parent chitosan presented a low average degree of acetylation ($\overline{DA}$ = 5%) and its reaction with myristoyl chloride occurred predominantly at the hydroxyl sites (Silva et al., 2017), the chains of the DMCh derivative are

Table 1
Values of average size, polydispersity index (PDI), zeta potential and encapsulation efficiency of DMCh micelles.

Sample	CPT (μg)	DMCh parameters[a]			
		Average diameter (nm)	PDI	Zeta potential (mV)	EE (%)[b]
DMCh **	0	326.67 ± 35.44	0.49 ± 0.06	29.57 ± 3,26	–
DMCh/CPT1	50	281.72 ± 16.55	0.49 ± 0.04	42.54 ± 2.12	100*
DMCh/CPT2	100	289.35 ± 38.38	0.44 ± 0.04	46.11 ± 0.21	69.97 ± 0.95
DMCh/CPT3	150	335.61 ± 16.23	0.44 ± 0.16	49.60 ± 4.17	41.55 ± 0.91

[a] Average size, dispersity and zeta potential were determined by dynamic light scattering.
[b] Encapsulation efficiency.

rich in amino groups, generating a high positive charge density upon protonation.

Thus, the high positive charge density at the hydrophilic shell of DMCh micelles strongly contributes to stabilize them and it also favors the interaction of the micelles with the negatively charged cell wall, resulting in enhanced absorption and penetration of CPT. The TEM images showed that DMCh/CPT2 micelles exhibited a regular spherical shape, they are well dispersed and no aggregation is observed (Fig. 2). However, it is possible to observe in Fig. 2 the presence of micelles smaller than 280 nm and a broad particle size distribution, a fact that corroborates the values of PDI (Table 1), characteristic of the polymer of random molecular weight and of the myristoyl groups added along the chain (Hickey, Santos, Williford, & Mao, 2015; Rao & Geckeler, 2011). Another reason for the apparent discrepancy of the data from DLS experiments and the TEM image lies in the fact that the former refer to the average hydrodynamic diameter of the swollen DMC micelles suspended in aqueous medium while the latter correspond to micelles which were previously submitted to drying process to allow the acquisition of the images.

The values of encapsulation efficiency (EE%) of CPT by DMCh micelles as a function of CPT theoretical loading are also shown in Table 1. These data show that EE% decreased with increasing CPT concentration, the maximum encapsulation efficiency being achieved when the lowest load of CPT was used. Such a result suggests that the capacity of DMCh micelles to encapsulate CPT may depend on the $\overline{DS}$ of the chitosan derivative, *i.e.* the encapsulation efficiency is limited by the content of myristoyl substituents along the polymer chains. Thus, taking into account the low content of myristoyl moieties in the DMCh chains ($\overline{DS}$ = 6.8%), the reduced CPT loading observed at high drug loadings may be attributed to the low density of polymer hydrophobic segments in the core of DMCh micelles.

However, the choice of the DMCh derivative with low average degree of substitution ($\overline{DS}$ = 6.8%) aimed to avoid the exposure of hydrophobic segments of DMCh chains at the micelles surface. Indeed, the exposure of the hydrophobic moieties at the micelles surface, which occurs if DMCh contains a higher content of substituents ($\overline{DS}$ > 10%), may affect the stability of the micellar system by decreasing the surface charge. Additionally, some drug may be entrapped at these hydrophobic domains at the micelles surface, affecting the encapsulation efficiency, exposing the drug located at these regions to degradation before releasing and increasing the cytotoxicity of the DMCh/drug delivery system.

In fact, micelles constituted by amphiphilic derivatives of chitosan presenting $\overline{DS}$ > 10% display higher drug loading capacity (Duan et al., 2010; Opanasopit et al., 2006, 2007; Pan et al., 2013; Woraphatphadung, Sajomsang, Gonil, Saesoo, & Opanasopit, 2015; Zhang et al., 2008; Zhang et al., 2007a, 2007b). However, besides the high loading capacity, carrier systems must be effective and present low toxicity to not impair the patient's quality of life (Gao et al., 2014). Thus, as already mentioned, the micellar system formed by the DMCh derivative presenting low $\overline{DS}$ was selected for this study, *i.e.* to avoid the exposure of the hydrophobic groups at the surface of the micelles while presenting low cytotoxicity.

3.3. In vitro CPT release study

CPT release profile from DMCh micelles was evaluated in simulated gastric and intestinal fluids. The release profile of free CPT and DMCh/CPT2 in the first 2 h (SGF; pH 1.2) and over a longer period (SIF; pH 6.8) are presented in Fig. 3a while the experimental data concerning only 4 h of experiment are shown in Fig. 3b. In the case of free CPT, about 90% of the total drug load was released after 8 h and a nearly complete release was observed after 12 h while only 21% of the total CPT load was released from DMCh/CPT2 micelles in the same time interval. In fact, the CPT loaded in DMCh/CPT2 micelles was rapidly released during the first hour, followed by a controlled release until the end of the experiment. A pH-dependent release of CPT from DMCh/CPT2 micelles was not evident, the drug release appearing to be continuous regardless of the medium pH until 2 h while from then on a linear and constant release ranging as 20–24% of the total CPT load was observed in SIF. The fact that CPT is released in an early stage may be convenient as it is important to guarantee enough drug concentration at the target sites to reach the desired therapeutic efficacy (Dinarvand et al., 2015). Thus, the results of *in vitro* CPT release study showed that DMCh micelles are suitable carriers of CPT, which can be sustainably released at the desired target.

3.4. In vitro cytotoxicity assay of CPT-loaded

In accordance with the results presented previously, the CPT-loaded

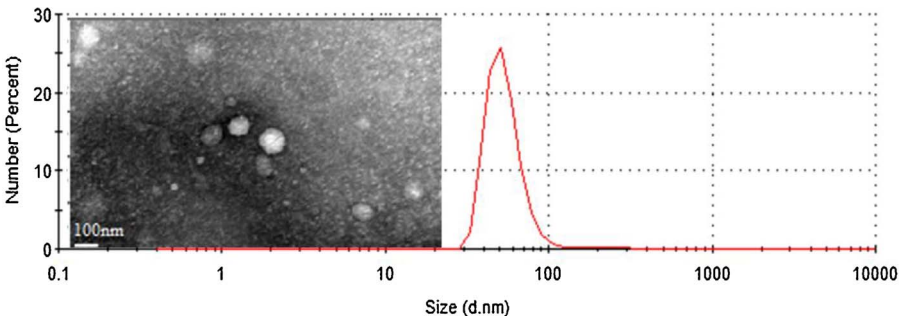

Fig. 2. TEM images and particle size distribution by number of DMCh/CPT2.

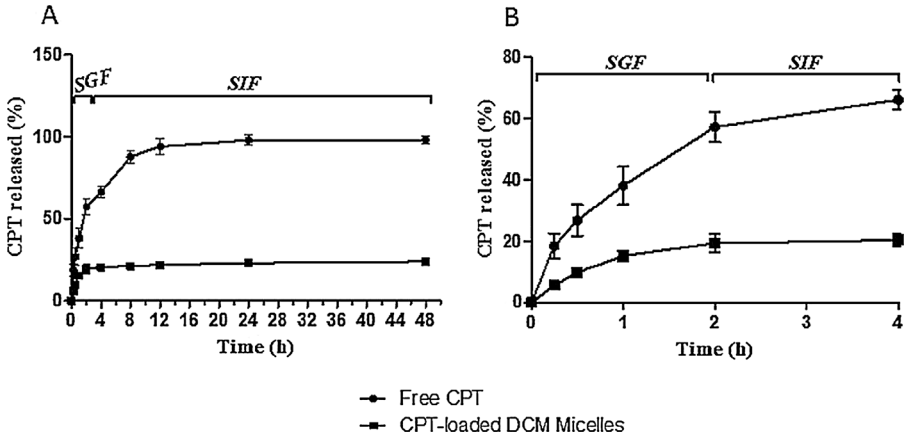

Fig. 3. Camptothecin release profile after incubation in simulated gastric fluid (SGF) (0–2 h) and simulated intestinal fluid (SIF) (2–48 h) under sink conditions at 37 °C. A) Data corresponding to the release profile over 48 h and B) Data corresponding to the release profile over 4 h. Data expressed as Mean ± SD, n = 3.

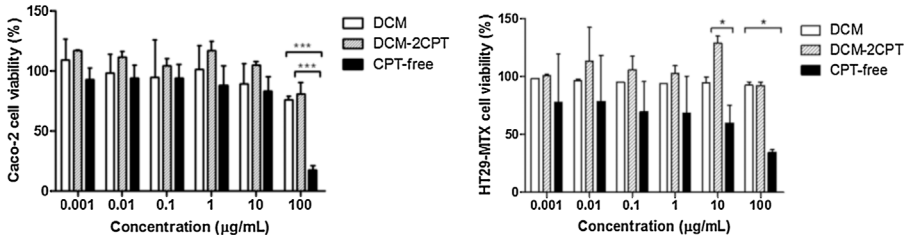

Fig. 4. Cytotoxicity of DMCh, DMCh/CPT2 and free CPT against Caco-2 and HT29-MTX cells line as a function of concentration (0.001–100 µg/mL). Values were reported as Mean ± SD (n = 3). (*) and (**) denotes a significant difference ($p < 0.05$ and $p < 0.01$, respectively).

micelle chosen to carry out the biological assay was DMCh/CPT2 due to its higher capacity of encapsulation and solubilization of CPT. The *in vitro* cytotoxicity of DMCh, DMCh/CPT2 and free CPT was evaluated in Caco-2 and HT29-MTX intestinal epithelial cell lines by the MTT assay (Fig. 4). Results of cell viability after 24 h of incubation in the presence of increasing concentrations of DMCh, DMCh/CPT2 and free CPT are shown in Fig. 4. It is possible to observe that DMCh did not present toxic effects toward none cell line in the range of concentrations evaluated, showing its potential to be used in the preparation of micelles intended to delivery drugs to the intestine. At low concentrations (≤10 mg/mL), cell viabilities were found to be higher than 80% for all concentrations of free CPT and CPT-loaded DMCh micelles. However, cell viability of both cell lines decreased significantly after the incubation with 100 µg/mL of free CPT. Nevertheless, this amount of CPT loaded into the DMCh micelles did not decrease the cell viability of Caco-2 or HT29-MTX, showing the ability of these micelles in reducing the drug toxicity. These results are in agreement with other studies performed with similar concentrations and using the same cell lines as well as other cell lines (Duan et al., 2010; Kolhatkar et al., 2008; Omar, Bardoogo, Corem-salkmon, & Mizrahi, 2016).

The HT29-MTX cell line presented higher sensitivity to free CPT when compared with Caco-2 model. The results also showed that DMCh and DMCh/CPT2 micelles have not exhibited cytotoxicity, but free CPT has displayed considerable toxicity. Moreover, such results showed that besides being atoxic the DMCh micelles significantly reduced the toxic effects of CPT.

Indeed, the DMCh-CPT2 micelles developed here showed lower toxicity compared to different chitosan-based CPT nanocarriers (Mathiyalagan, Subramaniyam, Kim, Kim, & Yang, 2014; Tahvilian, Tajani, Sadrjavadi, & Fattahi, 2016; Tang, Song, Chen, Wang, & Wang, 2013). Sun and coworkers reported CPT nanocolloids based on *N, N, N*-trimethyl chitosan as a potential system for the effective treatment of multiple myeloma (Sun et al., 2015). A commercial *N, N, N*-trimethyl chitosan sample was used in this study and no information on its average degree of substitution was given even though it strongly affects the polymer solubility, charge density and cytotoxicity (dos Santos, Bukzem, & Campana-Filho, 2016; Senra, Santos, Desbrières, & Campana-Filho, 2015). Additionally, this chitosan derivative results from the reaction of *N*-methylation of chitosan, which is generally carried out by using iodomethane in large excess, an alkylating agent that can cause damage to the lungs, liver, kidneys and central nervous system (Jintapattanakit, Mao, Kissel, & Junyaprasert, 2008; Stepnova et al., 2007; Xu, Xin, Li, Huang, & Zhou, 2010).

Tahvilian et al. inserted CPT into water-soluble chitosan oligosaccharide (CHO) using cis-aconityl (CA). However, the synthetic route to produce this chitosan derivative is complex as it involves two reaction steps, the use of labile reactants and of nitrogen atmosphere and low temperature (−20 °C). Additionally, this chitosan oligosaccharide derivative exhibited higher toxicity as compared to DMCh. Thus, comparing 3,6-*O*,*O*'-dimyristoyl chitosan to other chitosan derivatives employed to develop CPT carriers reveals that it is easier to be prepared in a single reaction step, carried out at room temperature for short time and its average degree of substitution can be controlled by properly adjusting the molar ratio chitosan/dimyristoyl chloride.

3.5. Permeability tests

The permeability of CPT across intestinal epithelial cells was studied, the main goal of this experiment being to investigate how DMCh micelles can improve CPT permeability. Thus, it was used a monoculture model constituted by Caco-2 cells, which represents the standard model that mimics human enterocytes. Additionally, the Caco-2/HT29-MTX co-culture model was used for being more similar to human intestine than Caco-2 cells alone, as HT29-MTX are mucus-secreting cells.

As depicted in Fig. 5, CPT-loaded DMCh micelles showed a different behavior when compared to free CPT. The P_{app} found for DMCh micelles was 3.6×10^{-6} cm/s and 8.2×10^{-6} cm/s for Caco-2 and Caco-2/HT29-MTX models, respectively. This high permeability coefficients obtained for DMCh micelles improved CPT permeability across epithelial cells up to four to eightfold in monoculture and co-culture models, respectively. In addition to the permeability improvement when compared with free CPT, the Caco-2/HT29-MTX model increased twofold CPT permeability from micelles. This might be attributed to the mucoadhesiveness of chitosan, which is due to the presence of positively charged ammonium groups along its chains, favoring the

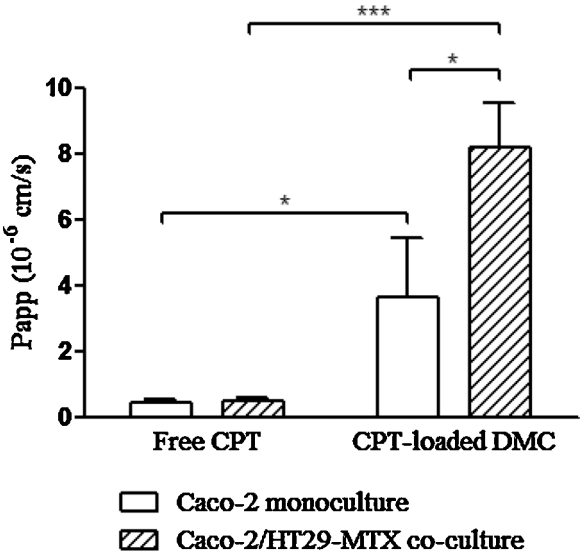

Fig. 5. Apparent permeability coefficients (Papp) of CPT-loaded micelles and free CPT across Caco-2 monoculture model (empty columns) and across Caco-2/HT29-MTX co-culture model (filled columns). All experiments were conducted from the apical to basolateral compartment in HBSS at 37 °C. Error bars represent Mean ± SD (n = 3).

interactions between DMCh micelles and the mucus produced by HT29-MTX cells and improving CPT permeability across the intestinal barrier, in agreement with our previous work (Silva et al., 2017). Indeed, other studies already reported that chitosan may interact with mucus layer of cell barriers (Mo et al., 2011; Yuan, Lu, Du, & Hu, 2010). In addition, it has been reported that chitosan is able to temporally open the tight junctions of epithelial cells, improving the permeability across intestinal barrier (Yeh et al., 2011).

Additionally, it was possible to observe that after 180 min, the CPT permeability reached 13% and 30% at the highest CPT concentration tested by using the Caco-2 monoculture and Caco-2/HT29-MTX co-culture models, respectively. Moreover, the CPT permeability occurred steadily throughout the experiment with high TEER values. The TEER values are an indicator of the integrity of cellular barriers and, therefore, they were monitored during all the experiment. Furthermore, the co-culture model presents lower TEER values when compared with the standard model, due to the presence of HT29-MTX cells. The tightness of HT29-MTX cells is lower than that of Caco-2, depicting lower TEER values, which can lead to a higher drug permeability (Araújo & Sarmento, 2013). In fact, it was observed a twofold increase in CPT permeability due to the presence of these characteristic tight junctions on HT29-MTX cells combined with the mucus produced in interaction with the chitosan-based mucoadhesive micelles. In case of free CPT, the results showed a decrease on TEER values to approximately 70%. Indeed, this decrease did not affect CPT permeability as evidenced in Fig. 6.

Overall, self-assembled chitosan-based micelles can significantly increase CPT *in vitro* permeability across human intestine, especially in the model that closely mimics the human intestine. These findings may be useful to improve bioavailability of hydrophobic drugs in cancer therapy after oral administration.

4. Conclusion

The self-aggregation behavior of 3,6-*O,O'*-dimyristoyl chitosan (DMCh) chains in aqueous medium results in the formation of micelles displaying core/shell architecture, which are able to encapsulate camptothecin (CPT), a water-insoluble hydrophobic anticancer agent, into its hydrophobic core. The CPT-loaded nano-sized micelles (281 nm–357 nm) are stabilized by repulsive electrostatic forces due to the presence of numerous positive charges at the hydrophilic shell of the DMCh micelles, owing to the protonation of amino groups pertaining to 2-amino-2-deoxy-D-glupyranose units. The encapsulation efficiency (EE) of CPT into DMCh micelles depends on the average degree of substitution ($\overline{DS}$) of the chitosan derivative, its low content of myristoyl substituents ($\overline{DS}$ = 6.8%) limiting the maximum CPT load of approximately 70 μg into DMCh micelles. The *in vitro* release of CPT from DMCh/CPT2 micelles is not pH-dependent and a sustained release is observed after 2 h, supporting the proposal of DMCh micelles as suitable carriers for oral administration of CPT. Empty DMCh micelles exhibit very low toxicity and although free CPT displays high toxicity toward Caco-2 and HT29-MTX intestinal epithelial cell lines at concentration 100 μg/mL, its encapsulation into DMCh micelles strongly decreases the drug toxicity, improving the safety of the oral administration of CPT. Owing to the mucoadhesiveness of DMCh/CPT2 micelles, which is mainly due to its largely positive zeta potential (> 30 mV), they are able to interact with the negatively charged mucus produced by HT29-MTX cells and to open temporarily the cell tight junctions, improving the *in vitro* permeability of CPT across intestinal barrier and enhancing its bioavailability. The whole set of results clearly indicate the potential of DMCh micelles to encapsulate and safely release camptothecin *via* oral administration.

Acknowledgments

The authors are also grateful to CAPES, CNPq, FAPESP, IQSC/USP for financial support. This work was financed by FEDER–Fundo Europeu de Desenvolvimento Regional funds through the COMPETE 2020–Operacional Programme for Competitiveness and Internationalisation (POCI), Portugal 2020 (NORTE-01-0145-FEDER-000012), and by Portuguese funds through FCT – Fundação para a Ciência e a Tecnologia/Ministério da Ciência, Tecnologia e Inovação in the framework of the project "Institute for Research and Innovation in

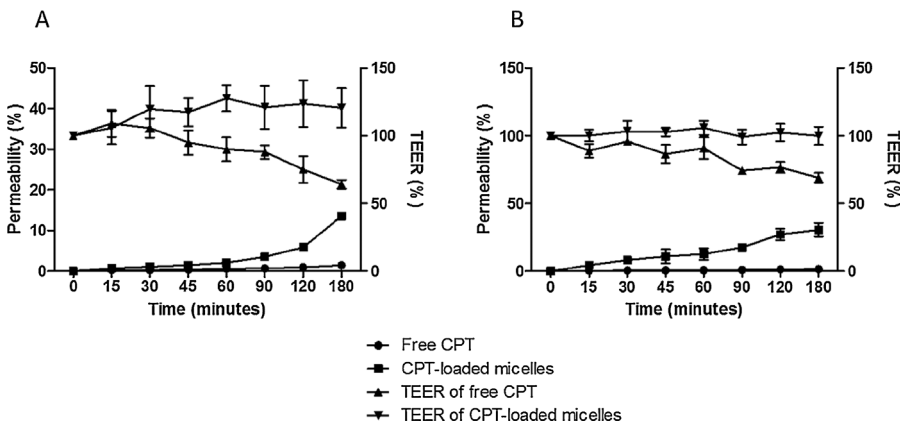

Fig. 6. *In vitro* cumulative permeability profile of CPT-loaded micelles (■) and free CPT (●) across Caco-2 monoculture model (A) and Caco-2/HT29-MTX co-culture model (B). All experiments were conducted from the apical to basolateral compartment in HBSS at 37 °C. Error bars represent Mean ± SD (n = 3).

Health Sciences" (POCI-01-0145-FEDER-007274). This research was also partially supported by CESPU/IINFACTS under the project MicelCampt-CESPU-2017.

References

Antunes, F., Andrade, F., Araújo, F., Ferreira, D., & Sarmento, B. (2013). Establishment of a triple co-culture in vitro cell models to study intestinal absorption of peptide drugs. *European Journal of Pharmaceutics and Biopharmaceutics, 83*(3), 427–435.

Araújo, F., & Sarmento, B. (2013). Towards the characterization of an in vitro triple co-culture intestine cell model for permeability studies. *International Journal of Pharmaceutics, 458*(1), 128–134.

Badawy, M. E. I., Rabea, E. I., Rogge, T. M., Stevens, C. V., Smagghe, G., Steurbaut, W., & Ho, M. (2004). Synthesis and fungicidal activity of new N, O-acyl chitosan derivatives. *Biomacromolecules,* 589–595.

Badawy, M. E. I., Rabea, E. I., Rogge, T. M., Stevens, C. V., Steurbaut, W., Höfte, M., & Smagghe, G. (2005). Fungicidal and insecticidal activity of O-acyl chitosan derivatives. *Polymer Bulletin, 54*(4–5), 279–289.

Choi, C. Y., Kim, S. B., Pak, P. K., Yoo, D. I., & Chung, Y. S. (2007). Effect of N-acylation on structure and properties of chitosan fibers. *Carbohydrate Polymers, 68*(1), 122–127.

Concheiro, A. (2010). Polymeric micelles as drug stabilizers: The camptothecin and simvastatin cases. *Journal of Drug Delivery Science and Technology, 20*(4), 249–257.

dos Santos, D. M., Bukzem, A. de L., & Campana-Filho, S. P. (2016). Response surface methodology applied to the study of the microwave-assisted synthesis of quaternized chitosan. *Carbohydrate Polymers, 138*, 317–326.

Delmar, K., & Bianco-Peled, H. (2016). Composite chitosan hydrogels for extended release of hydrophobic drugs. *Carbohydrate Polymers, 136*, 570–580.

Di Martino, A., & Sedlarik, V. (2014). Amphiphilic chitosan-grafted-functionalized polylactic acid based nanoparticles as a delivery system for doxorubicin and temozolomide co-therapy. *International Journal of Pharmaceutics, 474*(1–2), 134–145.

Dinarvand, M., Kiani, M., Mirzazadeh, F., Esmaeili, A., Mirzaie, Z., Soleimani, M., ... Atyabi, F. (2015). Oral delivery of nanoparticles containing anticancer SN38 and hSET1 antisense for dual therapy of colon cancer. *International Journal of Biological Macromolecules, 78*, 112–121. http://dx.doi.org/10.1016/j.ijbiomac.2015.03.066 Retrieved from.

Duan, K., Zhang, X., Tang, X., Yu, J., Liu, S., Wang, D., ... Huang, J. (2010). Fabrication of cationic nanomicelle from chitosan- graft −polycaprolactone as the carrier of 7-ethyl-10-hydroxy-camptothecin. *Colloids and Surfaces B: Biointerfaces, 76*, 475–482.

Ebrahim Attia, A. B., Ong, Z. Y., Hedrick, J. L., Lee, P. P., Ee, P. L. R., Hammond, P. T., & Yang, Y.-Y. (2011). Mixed micelles self-assembled from block copolymers for drug delivery. *Current Opinion in Colloid & Interface Science, 16*(3), 182–194.

Feng, T., Tian, H., Xu, C., Lin, L., Xie, Z., Lam, M. H. W., ... Chen, X. (2014). Synergistic co-delivery of doxorubicin and paclitaxel by porous PLGA microspheres for pulmonary inhalation treatment. *European Journal of Pharmaceutics and Biopharmaceutics, 88*(3), 1086–1093. http://dx.doi.org/10.1016/j.ejpb.2014.09.012.

Fiamingo, A., Delezuk, J. A. D. M., Trombotto, S., David, L., & Campana-Filho, S. P. (2016). Extensively deacetylated high molecular weight chitosan from the multistep ultrasound-assisted deacetylation of beta-chitin. *Ultrasonics Sonochemistry, 32*, 79–85.

Gao, J., Ming, J., He, B., Fan, Y., Gu, Z., & Zhang, X. (2008). Preparation and characterization of novel polymeric micelles for 9-nitro-20(S)-camptothecin delivery. *European Journal of Pharmaceutical Sciences: Official Journal of the European Federation for Pharmaceutical Sciences, 34*(2–3), 85–93.

Gao, Y., Xie, J., Chen, H., Gu, S., Zhao, R., Shao, J., & Jia, L. (2014). Nanotechnology-based intelligent drug design for cancer metastasis treatment. *Biotechnology Advances, 32*(4), 761–777.

Ge, Y., Ma, Y., & Li, L. (2016). The application of prodrug-based nano-drug delivery strategy in cancer combination therapy. *Colloids and Surfaces B: Biointerfaces, 146*, 482–489. http://dx.doi.org/10.1016/j.colsurfb.2016.06.051.

Gonzalez-alvarez, M., Rodríguez-berna, G., Mangas-sanju, V., & García-gim, L. (2014). A promising camptothecin derivative: semisynthesis, antitumor activity and intestinal permeability. *European Journal of Medicinal Chemistry Journal, 83*, 366–373.

Greco, F., & Vicent, M. J. (2009). Combination therapy: opportunities and challenges for polymer-drug conjugates as anticancer nanomedicines. *Advanced Drug Delivery Reviews, 61*(13), 1203–1213. http://dx.doi.org/10.1016/j.addr.2009.05.006.

Heux, L., Brugnerotto, J., Desbrières, J., Versali, M. F., & Rinaudo, M. (2000). Solid state NMR for determination of degree of acetylation of chitin and chitosan. *Biomacromolecules, 1*(4), 746–751.

Hickey, J. W., Santos, J. L., Williford, J. M., & Mao, H. Q. (2015). Control of polymeric nanoparticle size to improve therapeutic delivery. *Journal of Controlled Release, 219*, 535–547.

Hirano, S., Yamaguchi, Y., & Kamiya, M. (2002). Novel N-saturated-fatty-acyl derivatives of chitosan soluble in water and in aqueous acid and alkaline solutions. *Carbohydrate Polymers, 48*, 203–207.

Hu, Y., Du, Y., Yang, J., Tang, Y., Li, J., & Wang, X. (2007). Self-aggregation and antibacterial activity of N-acylated chitosan. *Polymer, 48*(11), 3098–3106.

Huarte, J., Espuelas, S., Lai, Y., He, B., Tang, J., & Irache, J. M. (2016). Oral delivery of camptothecin using cyclodextrin/poly (anhydride) nanoparticles. *International Journal of Pharmaceutics, 506*, 116–128.

Hyun, K., Park, K., Kim, Y., Mun, S., Lee, S., Gon, H., ... Chan, I. (2008). Hydrophobically modified glycol chitosan nanoparticles-encapsulated camptothecin enhance the drug stability and tumor targeting in cancer therapy. *Journal of Controlled Release, 127*, 208–218.

Jiang, G.-B. B., Quan, D., Liao, K., & Wang, H. (2006). Novel polymer micelles prepared from chitosan grafted hydrophobic palmitoyl groups for drug delivery. *Molecular Pharmaceutics, 3*(2), 152–160.

Jintapattanakit, A., Mao, S., Kissel, T., & Junyaprasert, V. B. (2008). Physicochemical properties and biocompatibility of N-trimethyl chitosan: Effect of quaternization and dimethylation. *European Journal of Pharmaceutics and Biopharmaceutics, 70*(2), 563–571. http://dx.doi.org/10.1016/j.ejpb.2008.06.002.

Johnson, R. L., & Schmidt-Rohr, K. (2014). Quantitative solid-state 13C NMR with signal enhancement by multiple cross polarization. *Journal of Magnetic Resonance, 239*, 44–49.

Kawano, K., Watanabe, M., Yamamoto, T., & Yokoyama, M. (2006). Enhanced antitumor effect of camptothecin loaded in long-circulating polymeric micelles. *Journal of Controlled Release, 112*, 329–332.

Kolhatkar, R. B., Swaan, P., & Ghandehari, H. (2008). Potential oral delivery of 7-ethyl-10-hydroxy-camptothecin (SN-38) using poly (amidoamine) dendrimers. *Pharmaceutical Research, 25*(7).

Laskar, P., Samanta, S., Kumar, S., & Dey, J. (2014). evaluation of pH-sensitive cholesterol-containing stable polymeric micelles for delivery of camptothecin. *Journal of Colloid and Interface Science, 430*, 305–314.

Maeda, H. (2001). The enhanced permeability and retention (EPR) effect in tumor vasculature: The key role of tumor-selective macromolecular. *Advances in Enzyme Regulation, 41*(0), 189–207.

Martins, S. M., Wendling, T., Gonc, V. M. F., Sarmento, B., Ferreira, D. C., Gonçalves, V. M. F., ... Ferreira, D. C. (2012). Development and validation of a simple reversed-phase HPLC method for the determination of camptothecin in animal organs following administration in solid lipid nanoparticles. *Journal of Chromatography B: Analytical Technologies in the Biomedical and Life Sciences, 880*(1), 100–107.

Mathiyalagan, R., Subramaniyam, S., Kim, Y. J., Kim, Y. C., & Yang, D. C. (2014). Ginsenoside compound K-bearing glycol chitosan conjugates: Synthesis, physicochemical characterization, and in vitro biological studies. *Carbohydrate Polymers, 112*, 359–366. http://dx.doi.org/10.1016/j.carbpol.2014.05.098.

Mi, Z., & Burke, T. G. (1994). Differential interactions of camptothecin lactone and carboxylate forms with human blood components. *Biochemistry, 33*(614), 10325–10336. http://dx.doi.org/10.1021/bi00200a013.

Mo, R., Jin, X., Li, N., Ju, C., Sun, M., Zhang, C., & Ping, Q. (2011). The mechanism of enhancement on oral absorption of paclitaxel by N-octyl-O-sulfate chitosan micelles. *Biomaterials, 32*(20), 4609–4620.

Omar, R., Bardoogo, Y. L., Corem-salkmon, E., & Mizrahi, B. (2016). Amphiphilic star PEG-Camptothecin conjugates for intracellular targeting. *Journal of Controlled Release Journal*.

Opanasopit, P., Yokoyama, M., Watanabe, M., Kawano, K., Maitani, Y., & Okano, T. (2005). Influence of serum and albumins from different species on stability of camptothecin-loaded micelles. *Journal of Controlled Release, 104*(2), 313–321. http://dx.doi.org/10.1016/j.jconrel.2005.02.014.

Opanasopit, P., Ngawhirunpat, T., & Chaidedgumjorn, A. (2006). Incorporation of camptothecin into N −phthaloyl chitosan-g-mPEG self-assembly micellar system. *European Journal of Pharmaceutics and Biopharmaceutics, 64*, 269–276.

Opanasopit, P., Ngawhirunpat, T., Rojanarata, T., Choochottiros, C., & Chirachanchai, S. (2007). Camptothecin-incorporating N −phthaloylchitosan-g-mPEG self-assembly micellar system: Effect of degree of deacetylation. *Colloids and Surfaces B: Biointerfaces, 60*, 117–124.

Ottøy, M. H., Vårum, K. M., & Smidsrød, O. (1996). Compositional heterogeneity of heterogeneously deacetylated chitosans. *Carbohydrate Polymers, 29*(1), 17–24.

Pagano, E., Borrelli, F., Izzo, A., Ungaro, F., Quaglia, F., & Bilensoy, E. (2015). Core −shell hybrid nanocapsules for oral delivery of camptothecin: Formulation development, in vitro and in vivo evaluation. *Journal of Nanoparticle Research, 17*(1), 42.

Pan, Z., Gao, Y., Heng, L., Liu, Y., Yao, G., Wang, Y., & Liu, Y. (2013). Amphiphilic N-(2,3-dihydroxypropyl)-chitosan-cholic acid micelles for paclitaxel delivery. *Carbohydrate Polymers, 94*(1), 394–399.

Parhi, P., Mohanty, C., & Sahoo, S. K. (2012). Nanotechnology-based combinational drug delivery: An emerging approach for cancer therapy. *Drug Discovery Today, 17*(17–18), 1044–1052. http://dx.doi.org/10.1016/j.drudis.2012.05.010.

Pavinatto, A., Souza, A. L., Delezuk, J. A. M., Pavinatto, F. J., Campana-Filho, S. P., & Oliveira, O. N. (2014). Interaction of O-acylated chitosans with biomembrane models: Probing the effects from hydrophobic interactions and hydrogen bonding. *Colloids and Surfaces B: Biointerfaces, 114*, 53–59.

Rao, J. P., & Geckeler, K. E. (2011). Polymer nanoparticles: Preparation techniques and size-control parameters. *Progress in Polymer Science, 36*(7), 887–913. http://dx.doi.org/10.1016/j.progpolymsci.2011.01.001.

Senra, T. D. A., Santos, D. M., Desbrières, J., & Campana-Filho, S. P. (2015). Extensive N −methylation of chitosan: Evaluating the effects of the reaction conditions by using response surface methodology: extensive N −methylation of chitosan. *Polymer International, 64*(11), 1617–1626.

Sgorla, D., Almeida, A., Azevedo, C., Jose, É., Sarmento, B., & Albuquerque, O. (2016). Development and characterization of crosslinked hyaluronic acid polymeric films for use in coating processes. *International Journal of Pharmaceutics, 511*(1), 380–389.

Shrestha, N., Shahbazi, M.-A., Araújo, F., Zhang, H., Mäkilä, E. M., Kauppila, J., ... Santos, H. A. (2014). Chitosan-modified porous silicon microparticles for enhanced permeability of insulin across intestinal cell monolayers. *Biomaterials, 35*(25), 7172–7179. Retrieved from http://www.ncbi.nlm.nih.gov/pubmed/24844163.

Silva, D. S., Almeida, A., Prezotti, F., Cury, B., Campana-Filho, S. P., & Sarmento, B. (2017). Synthesis and characterization of 3,6-O,O'- dimyristoyl chitosan micelles for oral delivery of paclitaxel. *Colloids and Surfaces B: Biointerfaces, 152*, 220–228.

Stepnova, E. A., Tikhonov, V. E., Babushkina, T. A., Klimova, T. P., Vorontsov, E. V., Babak, V. G., ... Yamskov, I. A. (2007). New approach to the quaternization of chitosan and its amphiphilic derivatives. *European Polymer Journal, 43*(6), 2414–2421. http://dx.doi.org/10.1016/j.eurpolymj.2007.02.028.

Sun, Lu, Li, Zhengguang, Li, Zhiyong, Gou, Maling, Qian, Zhiyong, & Peng, F. (2015).

Improving antitumor activity with N–Trimethyl chitosan entrapping camptothecin in colon cancer and lung cancer. *Journal of Nanoscience and Nanotechnology, 15*(9), 6397–6404.

Tahvilian, R., Tajani, B., Sadrjavadi, K., & Fattahi, A. (2016). Preparation and characterization of pH-sensitive camptothecin-cis-aconityl grafted chitosan oligosaccharide nanomicelles. *International Journal of Biological Macromolecules, 92*, 795–802. http://dx.doi.org/10.1016/j.ijbiomac.2016.07.100.

Tang, D.-L., Song, F., Chen, C., Wang, X.-L., & Wang, Y.-Z. (2013). A pH-responsive chitosan- *b* −poly(p-dioxanone) nanocarrier: Formation and efficient antitumor drug delivery. *Nanotechnology, 24*(14), 145101. http://dx.doi.org/10.1088/0957-4484/24/14/145101.

Tong, Y., Wang, S., Xu, J., Chua, B., & He, C. (2005). Synthesis of O,O′-dipalmitoyl chitosan and its amphiphilic properties and capability of cholesterol absorption. *Carbohydrate Polymers, 60*(2), 229–233.

Unsoy, G., Khodadust, R., Yalcin, S., Mutlu, P., & Gunduz, U. (2014). Synthesis of Doxorubicin loaded magnetic chitosan nanoparticles for pH responsive targeted drug delivery. *European Journal of Pharmaceutical Sciences, 62*, 243–250.

Wang, H., Zhao, Y., Wu, Y., Hu, Y., Lin Nan, K., Nie, G., & Chen, H. (2011). Enhanced antitumor efficacy by co-delivery of doxorubicin and paclitaxel with amphiphilic methoxy PEG-PLGA copolymer nanoparticles. *Biomaterials, 32*(32), 8281–8290. http://dx.doi.org/10.1016/j.biomaterials.2011.07.032.

Woraphatphadung, T., Sajomsang, W., Gonil, P., Saesoo, S., & Opanasopit, P. (2015). Synthesis and characterization of pH-responsive N-naphthyl-N, O-succinyl chitosan micelles for oral meloxicam delivery. *Carbohydrate Polymers, 121*, 99–106. http://dx.doi.org/10.1016/j.carbpol.2014.12.039.

Woraphatphadung, T., Sajomsang, W., Gonil, P., Treetong, A., Akkaramongkolporn, P., Ngawhirunpat, T., & Opanasopit, P. (2016). pH-Responsive polymeric micelles based on amphiphilic chitosan derivatives: Effect of hydrophobic cores on oral meloxicam delivery. *International Journal of Pharmaceutics, 497*(1–2), 150–160.

Wu, J. L., Wang, C. Q., Zhuo, R. X., & Cheng, S. X. (2014). Multi-drug delivery system based on alginate/calcium carbonate hybrid nanoparticles for combination chemotherapy. *Colloids and Surfaces B: Biointerfaces, 123*, 498–505. http://dx.doi.org/10.1016/j.colsurfb.2014.09.047.

Xu, T., Xin, M., Li, M., Huang, H., & Zhou, S. (2010). Synthesis, characteristic and antibacterial activity of N, N, N −trimethyl chitosan and its carboxymethyl derivatives. *Carbohydrate Polymers, 81*(4), 931–936. http://dx.doi.org/10.1016/j.carbpol.2010.04.008.

Xu, J., Strandman, S., Zhu, J. X. X., Barralet, J., & Cerruti, M. (2015). Biomaterials Genipin-crosslinked catechol-chitosan mucoadhesive hydrogels for buccal drug delivery. *Biomaterials, 37*, 395–404.

Ye, Y. Q., Yang, F. L., Hu, F. Q., Du, Y. Z., Yuan, H., & Yu, H. Y. (2008). Core-modified chitosan-based polymeric micelles for controlled release of doxorubicin. *International Journal of Pharmaceutics, 352*, 294–301.

Yeh, T. H., Hsu, L. W., Tseng, M. T., Lee, P. L., Sonjae, K., Ho, Y. C., & Sung, H. W. (2011). Mechanism and consequence of chitosan-mediated reversible epithelial tight junction opening. *Biomaterials, 32*(26), 6164–6173.

Yuan, H., Lu, L., Du, Y., & Hu, F. (2010). Stearic acid- g −chitosan polymeric micelle for oral drug delivery: In vitro transport and in vivo absorption. *Molecular Pharmaceutics, 8*(1), 225–238.

Zhang, C., Ding, Y., Lucy, L., & Ping, Q. (2007a). Polymeric micelle systems of hydroxycamptothecin based on amphiphilic N −alkyl- N −trimethyl chitosan derivatives. *Colloids and Surfaces B: Biointerfaces, 55*, 192–199.

Zhang, C., Ding, Y., Yu (Lucy), L., & Ping, Q. (2007b). Polymeric micelle systems of hydroxycamptothecin based on amphiphilic N-alkyl-N-trimethyl chitosan derivatives? *Colloids and Surfaces B: Biointerfaces, 55*(2), 192–199.

Zhang, C., Qu, G., Sun, Y., Wu, X., Yao, Z., Guo, Q., … Zhou, H. (2008). Pharmacokinetics, biodistribution, efficacy and safety of N-octyl-O-sulfate chitosan micelles loaded with paclitaxel. *Biomaterials, 29*(9), 1233–1241.

Zhao, X., Chen, Q., Li, Y., Tang, H., Liu, W., & Yang, X. (2015). Doxorubicin and curcumin co-delivery by lipid nanoparticles for enhanced treatment of diethylnitrosamine-induced hepatocellular carcinoma in mice. *European Journal of Pharmaceutics and Biopharmaceutics, 93*(March), 27–36. http://dx.doi.org/10.1016/j.ejpb.2015.03.003.

Zuñiga, A., Debbaudt, A., Albertengo, L., & Rodríguez, M. S. (2010). Synthesis and characterization of N-propyl-N-methylene phosphonic chitosan derivative. *Carbohydrate Polymers, 79*(2), 475–480.